LASER INTERFEROMETER GRAVITATIONAL WAVE OBSERVATORY

LIGO Laboratory / LIGO Scientific Collaboration

LIGO-T0900640-v1 *LIGO* December 17, 2009

Acceleration of the FFT simulation of stable cavity

Hiro Yamamoto

Distribution of this document:
LIGO Science Collaboration

This is an internal working note
of the LIGO Project.

California Institute of Technology
LIGO Project – MS 18-34
1200 E. California Blvd.
Pasadena, CA 91125
Phone (626) 395-2129
Fax (626) 304-9834
E-mail: info@ligo.caltech.edu

Massachusetts Institute of Technology
LIGO Project – NW17-161
175 Albany St
Cambridge, MA 02139
Phone (617) 253-4824
Fax (617) 253-7014
E-mail: info@ligo.mit.edu

LIGO Hanford Observatory
P.O. Box 1970
Mail Stop S9-02
Richland WA 99352
Phone 509-372-8106
Fax 509-372-8137

LIGO Livingston Observatory
P.O. Box 940
Livingston, LA 70754
Phone 225-686-3100
Fax 225-686-7189

http://www.ligo.caltech.edu/

1. Introduction

Second generation gravitational wave detectors using laser interferometry adopt stable cavity configuration in the recycling cavity. One realization is to place a mode matching telescope in the recycling cavity and makes the gouy phase of the recycling cavity large enough to suppress the degeneracy.

The field is focused to make the Rayleigh range small so that enough gouy phase is aquired through propagation in a limited length cavity. In the focusing cavity where mode parameter changes, the field curvature is small and the field exhibits very rapid oscillation in the plane perpendicular to the propagation direction. This makes it difficult to use a FFT-based simulation to calculate the field propagation through the cavity because the number of grid points needs to be large so that the initial boundary condition with rapid oscillation can be properly sampled.

An algorithm based on the adaptive grid size formulation of the FFT-based cavity simulation is shown to accelerate the calculation of fields propagating through a stable cavity adapted in the recycling cavity. This method allows the number of the grid points of the FFT calculation to be smaller than that needed when this algorithm is not used, and the simulation time can be reduced by an order of magnitude.

2. Focusing cavity

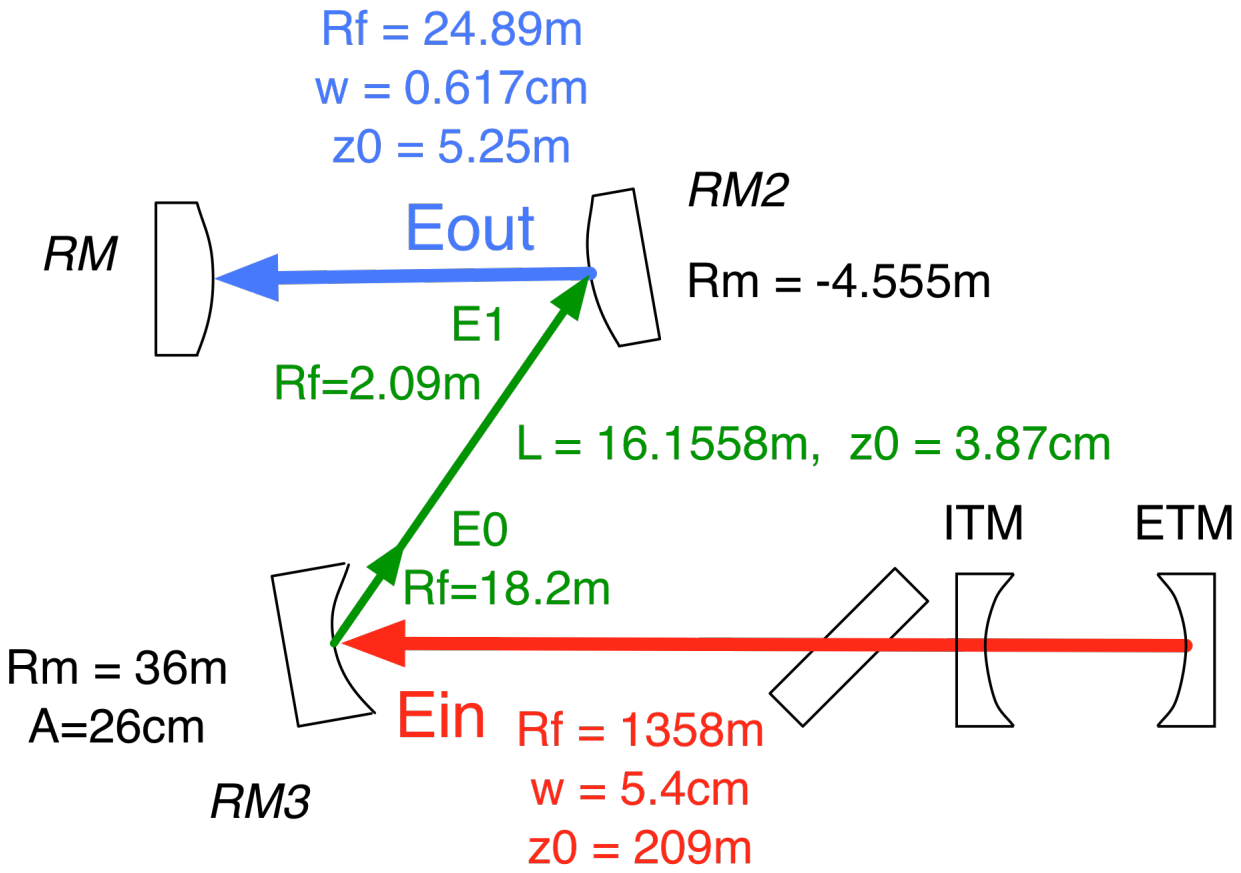

Figure 1 Focusing cavity

Figure 1 shows the recycling cavity consisted of a recycling mirror, RM, a focusing cavity made of RM2 (ROC=-4.555m) and RM3 (ROC=36m), and ITM. Ein is the field going to RM3, and its field parameters are shown in red. Ein is reflected by RM3 to E0, and E0 propagates to RM2 to become E1. E1 is then reflected by RM2 to become Eout, and its parameters are shown in blue. The focusing cavity length is 16.1558m and the Rayleigh range in the cavity is very small, 3.87cm. The dominant part of the gouy phase comes from the cavity formed by RM and RM2, which accounts for 95% of the total gouy phase of the recycling cavity, 25°.

The ROC of E0 is 100 times smaller than that of Ein, and the ROC of E1 is 10 times smaller than that of Eout. E0 and Ein (E1 and Eout) have the same beam size on the reflecting mirror, so the spatial oscillation of E0 (E1) is much rapid than Ein (Eout). This causes the numerical simulation difficult as is discussed below.

In this document, the discussion is limited to the propagation from Ein to Eout in Figure 1, but the same argument applies to the reverse propagation.

The Fresnel approximation of the Huygen's integral propagating from z0 to z1 is given by the convolution of the source field at z_0, and the paraxial propagation kernel:

$$E(x_1,y_1,z_1) = \iint dx_0 dy_0 E(x_0,y_0,z_0)\cdot K(\Delta x,\Delta y,\Delta z) \qquad \textbf{(1)}$$
$$\Delta x = x_1 - x_0,\ \Delta y = y_1 - y_0,\ \Delta z = z_1 - z_0$$

where K(x,y,z) is the paraxial propagation kernel defined as

$$K(x,y,z) = \frac{i}{z\cdot\lambda}\exp(-i\cdot k\cdot\frac{x^2+y^2}{2z}) \qquad (2)$$
$$r^2 = x^2 + y^2$$

When an incoming field, E_{in}, is reflected by a mirror with curvature R_m at normal incidence, the reflected field, E_0, acquires the following wave front phase:

$$E_0(x,y,z) = M_m(x,y,z)\cdot E_{in}(x,y,z)$$
$$= \overline{M_m}(x,y,z)\cdot E_{in}(x,y,z)\cdot\exp(i\cdot\phi(r)) \qquad \textbf{(3)}$$
$$\phi(r) = k\cdot\frac{r^2}{R_m}$$

In this equation, M_m is the effect of the reflection by the mirror m, and $\overline{M}_m$ is the part after removing the phase by its curvature which is explicitly written as exp(iϕ). M_m is 0 outside of the mirror aperture. The field curvature changes by $-R_m/2$ by this reflection. The reflection map $\overline{M}_m$ is assumed be smooth and can be handled using the same FFT grid spacing used for E_{in}.

The field propagating from RM3 to RM2 is calculated by substituting the source field E_0 given by Eq. (3) in the propagation formula Eq. (1). The integration goes over the mirror RM3 surface.

When the field E_0 on RM3 is sampled with a spacing of dr, the phase change from r to r+dr is

$$d\phi = \frac{2k\cdot r\cdot dr}{R_m} \qquad \textbf{(4)}$$

In order to change the Rayleigh range in a short distance, curvature of the focusing mirror is small. With R_m=36m and r=5.4cm, the phase spacing in units of 2π is

$$\frac{d\phi}{2\pi} = \frac{2 \cdot 0.054}{36 \cdot 1.064 \times 10^{-6}} dr = 2800 \cdot dr \qquad (5)$$

The FFT-based simulation uses data values at grid points on the mirror surface. In order to have enough sampling points, e.g., 10, at this radius, the spacing should be 3.6×10^{-5}m, or 9000 sampling points in a ±3 x beam size window. In the central region with smaller value of r, this number can be smaller, yet special care needs to be taken to use very large number of sampling points to properly handle this very rapid oscillation in the outer region.

3. Field propagation with magnification

When a field propagates from RM3 to RM2, the beam size becomes smaller by an order of magnitude. It was shown that a coordinate scaling is convenient to handle these cases [1, 2].

In order to magnify the beam size of E_1, the coordinate perpendicular to the propagation direction is scaled by a factor of α with the substitution of $x_1 = \alpha\, x_1'$ and $y_1 = \alpha\, y_1'$ in the propagation formula Eq. (1). With α < 1, the image size in the new coordinate system in (x_1', y_1') is magnified by 1/α.

By changing the arguments of the propagation kernel K from (x_1-x_0,y_1-y_0) to (x_1'-x_0,y_1'-y_0), the integral formula can be rewritten as follows:

$$\begin{aligned} E_1(x_1, y_1, z_1) &= \iint dx_0 dy_0 E_0(x_0, y_0, z_0) \cdot K(x_1 - x_0, y_1 - y_0, \Delta z) \\ &= \iint dx_0 dy_0 E_0(x_0, y_0, z_0) \cdot K(\alpha x_1' - x_0, \alpha y_1' - y_0, \Delta z) \\ &= \widetilde{C}(x_1, y_1, \Delta z, \alpha) \iint dx_0 dy_0 \widetilde{E}_0(x_0, y_0, z_0) \cdot K(x_1' - x_0, y_1' - y_0, \Delta z / \alpha) \end{aligned} \qquad (6)$$

where $\widetilde{E}$ and $\widetilde{C}$ are given as follows:

$$\begin{aligned} \widetilde{E_0}(x_0, y_0, z_0) &= E_0(x_0, y_0, z_0) \exp(i \cdot \phi_0(r_0)) \\ \phi_0(r) &= k \frac{(\alpha - 1)}{2\Delta z} r^2 \end{aligned} \qquad (7)$$

$$\begin{aligned} \widetilde{C}(x_1, y_1, \Delta z, \alpha) &= \frac{1}{\alpha} \exp(i \cdot \widetilde{\psi}(r_1)) \\ \widetilde{\psi}(r) &= k \frac{(1/\alpha - 1)}{2\Delta z} r^2 \end{aligned} \qquad (8)$$

When E_0 is replaced by the expression using E_{in}, Eq. (3), $\widetilde{E}$ becomes as follows:

$$\begin{aligned} \widetilde{E}_0(x_0, y_0, z_0) &= \overline{M}_{m3}(x_0, y_0, z_0) \cdot E_{in}(x_0, y_0, z_0) \exp(i \cdot \phi_{in}(r_0)) \\ \phi_{in}(r) &= k\left(\frac{(\alpha - 1)}{2\Delta z} + \frac{1}{R_{m3}}\right) r^2 \end{aligned} \qquad (9)$$

where R_{m3} is the ROC of and M_{m3} is the reflection map of RM3.

If α is chosen to be

$$\alpha = 1 - \frac{2\Delta z}{R_{m3}} \qquad (10)$$

the rapidly oscillating part in Eq. (3) is cancelled by the extra factor introduced by the coordinate scaling. The oscillation can be suppressed when α is close to this optimal value.

This optimal scaling factor α is a reasonable choice. The Rayleigh range in the focusing cavity is very small, and the beam size of a field is proportional to the distance to the waist position. The distance between RM3 and the waist position is $-R_{m3}/2$, and that of RM2 is $-R_{m3}/2 + \Delta z$ in this approximation, so the optimal choice of α, Eq. (10), is approximately the ratio of the beam size on RM2 to that on RM3.

Field E_{out} is related to E_1 by the following equation, similar to Eq.(3):

$$\begin{aligned} E_{out}(x,y,z) &= M_{m2}(x,y,z)\cdot E_1(x,y,z) \\ &= \overline{M_{m2}}(x,y,z)\cdot E_1(x,y,z)\cdot \exp(i\cdot\phi(r)) \\ \phi(r) &= k\cdot\frac{r^2}{R_{m2}} \end{aligned} \qquad \textbf{(11)}$$

where R_{m2} is the ROC of and M_{m2} is the reflection map of RM2. $\overline{M_m}$ is a part of the reflection map excluding the mirror curvature, and this includes the finite aperture and surface aberration effects.

By combining this with Eq.(6), the field E_{out} is related to E_{in} by the following equation:

$$E_{out}(x_1,y_1,z_1) = C(x_1,y_1,\Delta z,\alpha)\iint dx_0 dy_0 \widetilde{E}_0(x_0,y_0,z_0)\cdot K(x_1'-x_0,y_1'-y_0,\Delta z/\alpha) \qquad (12)$$

where C is defined as follows:

$$\begin{aligned} C(x_1,y_1,\Delta z,\alpha) &= \frac{1}{\alpha}\exp(i\cdot\psi(r_1))\cdot\overline{M}_{m2}(x_1,y_1,z_1) \\ \psi(r) &= k\left(\frac{(1/\alpha-1)}{2\Delta z}+\frac{1}{R_{m2}}\right)r^2 \end{aligned} \qquad (13)$$

If you use the optimal value of α, Eq.(10), then this relation becomes simplified as follows:

$$\begin{aligned} &E_{out}(x_1,y_1,z_1) = \\ &C(x_1,y_1,\Delta z,\alpha)\iint dx_0 dy_0 E_{in}(x_0,y_0,z_0)\cdot\overline{M}_{m3}(x_0,y_0,z_0)\cdot K(x_1'-x_0,y_1'-y_0,\Delta z/\alpha) \end{aligned} \qquad (14)$$

$$\begin{aligned} C(x_1,y_1,\Delta z,\alpha) &= \frac{1}{\alpha}\exp(i\cdot\psi(r_1))\cdot\overline{M}_{m2}(x_1,y_1,z_1) \\ \psi(r) &= k\left(\frac{1}{R_{m3}-2\Delta z}+\frac{1}{R_{m2}}\right)r^2 \end{aligned} \qquad (15)$$

Because $R_{m3} + R_{m2} - 2\Delta z \ll 2\Delta z$, $\psi(r)$ is much smaller than $\widetilde{\psi}(r)$ in Eq.(8) for arbitrary chosen value of α. This corresponds to the fact that the ROC of E_{out} is much larger than that of E_1. This relationship holds when α is close to the optimal value.

4. Propagation using FFT

Eq.(12) gives the expression to calculate the outgoing field, E_{out}, of the focusing cavity by using the incoming field, E_{in}. The rapidly oscillating phase ϕ in Eq.(3) and that in Eq. (11), can be suppressed by a proper choice of the scaling factor α. One optimal choice is the one given in Eq.(10), which makes ϕ_{in} to 0 and makes ψ in Eq.(13) suppressed as well.

Because the propagation formula to calculate the outgoing field is a convolution of the incoming field, reflection map with similar spatial structure and the propagation kernel, the size of the FFT grid can be the same as that for the incoming field.

The Fourier transformation of the integral part of Eq. (14) can be written as a product of the Fourier transformation of the product of the incoming field and the reflection map, $\widehat{E}_0$, and that of the propagation kernel with a propagation distance of $(z_1\text{-}z_0)/\alpha$, $\widehat{K}$.

$$E_{out}(x_1, y_1, z_1) = C(x_1, y_1, \Delta z, \alpha) \times \iint df_x\, df_y \widehat{E_0}(f_x, f_y, z_0) \cdot \widehat{K}(f_x, f_y, \Delta z/\alpha) \cdot \exp(-i2\pi(f_x x_1' + f_y y_1')) \quad (16)$$

The outgoing field is calculated in the following steps.

1) Calculate the source field using Eq.(9).
2) Using the propagation kernel, propagate the incoming field by $(z_1\text{-}z_0)/\alpha$, using FFT.
3) Scale the output coordinate by $1/\alpha$, i.e., switch the coordinate from (x_1', y_1') to (x_1, y_1).
4) Multiply $C(x_1, y_1, \Delta z, \alpha)$, Eq.(15).

So long as a proper value of α is chosen, the source field, Eq.(9), has similar spatial structure as the incoming field, no special care is needed when FFT is applied.

5. Practical issues

There are a few practical issues to apply this method.

First is the separation of the phase from the mirror reflection map. Mathematically, Eq.(12) can be expressed using M_m, instead of $\overline{M}_m$, together with ϕ_0 in Eq.(7). So long as α is chosen properly, large oscillations in these two functions cancel each other. But, numerically, it often happens that these oscillation phases are calculated in slightly different way, and that can introduce imperfect cancellation. So, it is better to use an expression which does not include any large oscillation.

Second is the chose of the scaling factor α. The product of two optimal scaling factors, α_{32} for the propagation from RM3 to RM2 and α_{32} for the propagation from RM2 to RM3, is

$$\alpha_{32} \cdot \alpha_{23} = 1 + \frac{4\Delta z^2}{R_{m3} R_{m2}} \left(1 - \frac{R_{m3} + R_{m2}}{2\Delta z}\right) \quad (17)$$

Because $R_{m2}+R_{m3} \neq 2\,\Delta z$, the scaling from RM3 to RM2 and RM2 to RM3 are not reciprocal. But it is close enough that the suppression of the oscillation is enough when one α is chosen to be reciprocal of the other, e.g., α(RM2 to RM3) = 1/ α32.

Usually, the optimal value of α will not give a convenient FFT window size or spacing on one side or both of the propagation. It may be convenient to use the optimal value of α for both propagations and apply a smooth interpolation to the FFT grid points which was set by the user.

6. Numerical results

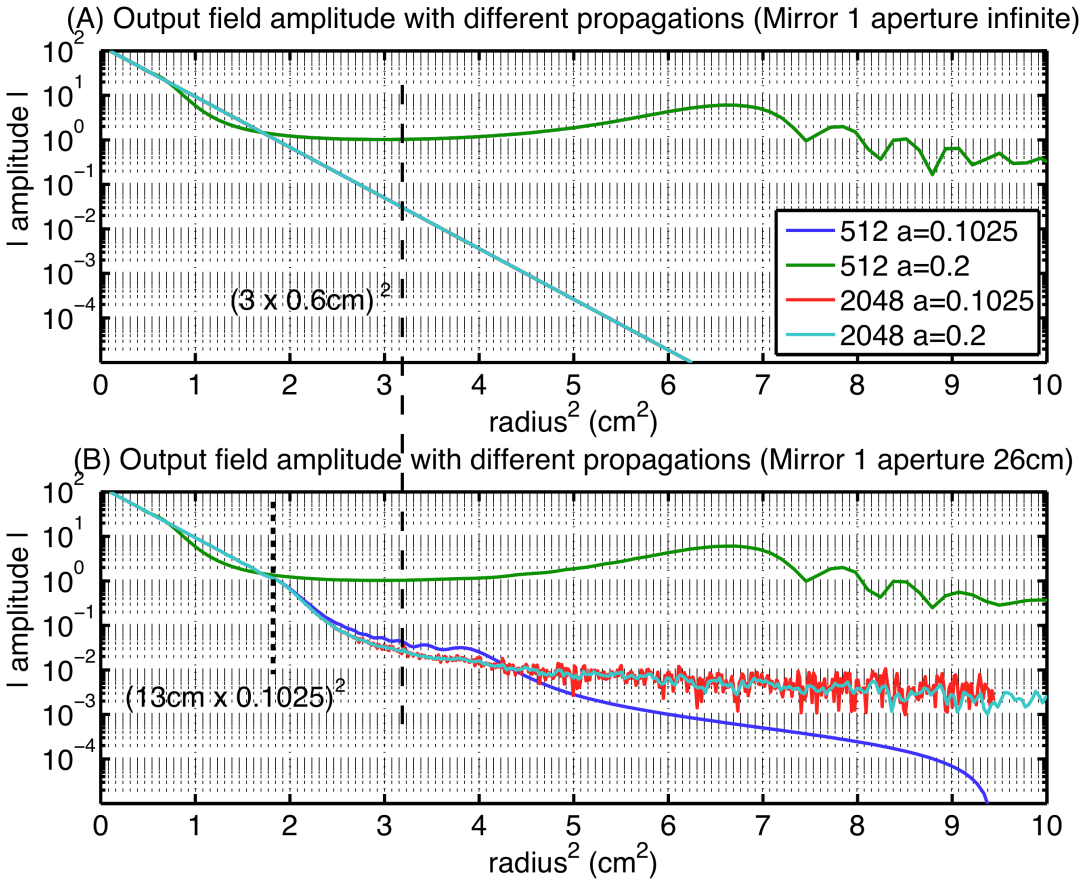

Figure 2 Propagation with different propagation
(In Fig.(A), 3 lines except green overlap each other)

This figure shows amplitudes of the field E_{out} for the same input field, E_{in}, TEM00(ROC=1358m,w=5.4cm), calculated using different propagation methods. Figure (A) is the case when the aperture of RM3 is infinite and (B) is the case when the aperture is 26cm. 512 or 2048 marks the number of FFT grid points. The FFT window size is 60cm on RM3, and the scaling factor α is the optimal value, 0.1025, and an arbitrary value, 0.2.

The beam size on RM2 is 0.6cm, and the 3 times of the beam size is shown by long a dashed line. As is shown in both (A) and (B), when an optimal value is chosen for the scaling factor, the number of grid points can be small (blue), compared to the case using an arbitrary scaling factor (green).

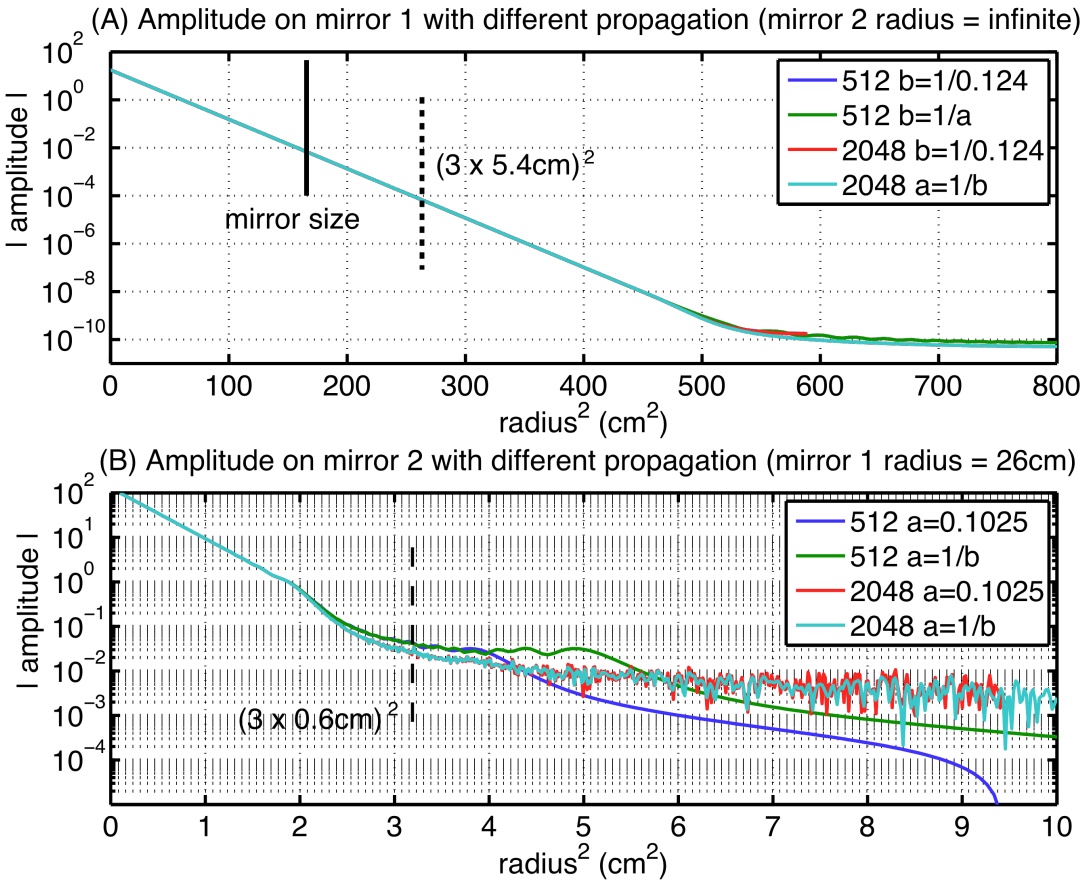

Figure 3 Choice of reciprocal value
(For the Fig.(A) calculation, PR3 mirror size is set to infinite to show the tail. The true reflected field will be cut at the line marked as mirror size.)

This figure shows the effect using a reciprocal value of α for one propagation.

Figure (A) is a case for the propagation from RM2 to RM3 (mirror 1 corresponds to RM2 and mirror 2 to RM3). The RM2 aperture is much larger than the beam size. 0.124 is the optimal scaling from RM2 to RM3 and b=1/a means that the scaling factor is calculated using the reciprocal of the scaling from RM3 to RM2, i.e., 1/0.1025. As is clear that the reciprocal value is close enough that 512 is good enough for the propagation.

Figure (B) is the propagation from RM3 to RM2 (mirror 1 is RM3 and mirror 2 is RM2). The aperture of RM3 is 26cm. Again, up to 3 times of the beam size, marked by long dashed line, 512 is good enough either the optimal value is used (blue) or the reciprocal (green, 1/0.124).

7. Summary

One needs to properly suppress the spatial oscillation due to the small ROC of the focusing mirrors. So long as the scaling factor is chose to make the oscillation to be small, the number of the FFT

grid points for the propagation through the focusing cavity can be as small as the one used for the propagation of fields outside of the focusing cavity.

8. References

1. The Virgo collaboration, "The Virgo Physics Book, Vol. II : OPTICS and related TOPICS", April 21, 2006
2. E. A. Sziklas and A. E. Siegman, "Mode calculations in unstable resonators with flowing saturable gain. 2: Fast Fourier transform method", Appl. Opt. 14, 1874-1889 (1975)